Website: www.gmrc.ca
Phone Number: 418-788-3017 / 418-788-3192
Email: marsenault@ginu.co

3rd April 2025

OVERVIEW

This paper will provide a thorough explanation and reasoning of the methodology for detecting the presence and severity of erosion (sediment input) from stream road crossings. This study focuses specifically on sediment input from forest roads, but the analysis will cover all road types due to the ease of expanding the analysis and recognizing that there are sediment inputs outside of forest roads inputs.

Background

Canada is the largest exporter of wood products in the world, due to Canada holding 9% of the Worlds' forests. Quebec contains 25% of the forests in Canada, which contribute to approximately 12% of the province's total exports (Statistics Canada, 2014). The forest industry in Quebec provides valuable economic benefits (Mobtaker et al., 2018), but comes at the cost of the need for forest roads that can cause direct and indirect effects to water quality, infiltration, sediment input, and habitat quality (Rice & Church, 2001; Boston, 2016; Kastridis, 2020)

With the continued rise of industrialization in the forest industry, the surface relief of catchments are being dramatically altered (Forman & Alexander, 1998; Wu et al., 2012). In remote forested areas, roads are elevated to maintain an equal gradient and reduce high flow events impact on those infrastructure. Drainage channels from developed landscapes such as forest roads and agricultural farms have a measurable impact on the surrounding water catchments (Forman & Alexander, 1998). Excessive sediment input into water catchments caused by erosion can cause infrastructure failure, habitat alteration and destruction (Simon & Rinaldi, 2000; Rice & Church, 2001) Erosion is a natural geomorphic process, but human alterations to the landscape can cause an increase in the scope, magnitude, and duration (Prosdocimi, et al., 2015).

Quebec installs approximately 10,000 culverts annually for recreational or forestry activities (FAPAQ, 2002). Culverts increase fine sediment input into the water course (Clarke & Scruton, 1997; Wellman et al., 2000). The accumulation of sediment can cause habitat alteration or destruction downstream, which can result in reproductive success, abundance, diversity, growth, and production of aquatic species (Argent & Flebbe, 1999; Scrimgeour et al., 2000; Williams et al., 2002).

When measuring impacts of forest roads and other anthropogenic developments, the variables to measure can vary depending on whether the project is carried out by forest land managers or conservationists. An example from Sheridan & Noske (2007) showed that forest land managers would be focused on variables such as intensity, frequency, and duration due to the temporal relationship between the mentioned variables and water quality. While a land manager would be concerned with variables such as loss of storage capacity.

Identifying stream crossings or road embankments that are prone to erosion are typically identified using field surveys through stream monitoring, sediment tracing, or roadside sediment traps. Roadside sediment traps are not used often due to finer sediments not being captured, variability in bedload inputs, and sediment yield (Robichaud & Brown, 2002). Sediment tracing can be useful for watershed scale analysis, but are influenced by water geochemistry (Wallbrink et al., 2002; Fu et al., 2010).

It is widely recognized that the alteration of our hydro-geomorphological functions can cause severe impacts on the surrounding environment (Forman & Alexander, 1998; Trombulak and Frissell 2001; Forman et al. 2003), the identification and assessment require field work (Biron et al., 2013). Carrying out field work over large landscapes without any prior knowledge of where to look can be a time sink, hazardous, and expensive (Kemp & O'Hanley, 2010; Marcus, 2012). These constraints have been alleviated in recent years through the adoption of airborne remote sensing data techniques, such as Light Detection and Ranging (LiDAR). High resolution LiDAR can produce topographic data with high vertical accuracy that can be transformed into models that represent the Earth's bare landscape surface, often referred to as a digital elevation model (DEM) (Lohani et al., 2017). Using LiDAR DEM's, managers can use topographic features from the LiDAR DEM to find vulnerable areas for field workers to further investigate (Telbisz et al., 2016).

Our goal for this project is to provide a scientific methodology in which we can identify erosion prone areas at a watershed scale, identify individual crossings within those erosion prone areas, identify and verify the sediment sources for each crossing for the entire Gaspe Peninsula. We chose the Cascapedia watershed to test and verify our methodology before expanding to the entire Peninsula. For this project, we have outlined 4 objectives to accomplish:

1. Identify erosion-prone areas using the Revised Universal Soil Loss Equation (RULSE).

2. Use the Sediment Transport Index to identify erosion-prone features for all individual stream-road crossings that are erosion-prone.

3. Field verification of our findings from the two above goals.

4. Project outcome

Methods

Study Area

We chose the Cascapedia watershed due to the variation in landscape morphology, the watershed size, and the diversity of land use (Figure 1).

Figure 1. Extent of the study area, the Cascapedia watershed located in Quebec, Canada.

The majority (X > 90%) of soil groups in the Gaspe Peninsula is classified under the soil group Humo-Ferric Podzol (HFP); an acidic coarse-to medium-textured soil group that is more vulnerable to mass sediment movements and erosion due to insufficient horizon development time (Zebarth et al., 2002). Additionally, the Gaspe Peninsula is characterized by numerous steep valleys, mountains, and agricultural land. The HFP soil group does not store water, has low organic carbon, and does not have cemented subsoil to facilitate drainage (Table 2), leading to increased agricultural disturbances to make the soil yield adequate crops (Shelton et al., 1985; Laverdiere et al., 1977). This leads to farmers to alter the soil by limestone, fertilizer or additional organic matter (Wang & Rees, 1980). Increased agricultural activity can increase erosion risk through not maintaining water erosion from intensively tilled crops (De Kimpe & Laverdiere, 1988).

Data sources

All data was sourced from public sources (Table 1), in the highest resolution available. Panagos et al. (2023) created a model that created a global rainfall erosivity raster at 1 meter resolution based on publicly available rainfall data.

Table 1. Variables used for sediment model, file type, resolution, source, and access URL

GIS Layer	Data Type	Data Source	Spatial Resolution	Source
LiDAR DEM	Raster	Données Quebec	1 meter	https://www.donneesquebec.ca/recherche/dataset/produits-derives-de-base-du-lidar
Road network	Feature	Données Quebec	-	https://www.donneesquebec.ca/recherche/dataset/reseau-routier-rtss
Stream network	Feature	Données Quebec/User generated	-	https://www.donneesquebec.ca/recherche/dataset/grhq
Rainfall Erosivity (R)	Raster	GloReda (Panagos et al., 2017-2023)	1 meter	https://www.sciencedirect.com/science/article/pii/S2352340923005826
Soil Erodibility (K)	Raster	Données Quebec	100 meter	https://www.donneesquebec.ca/recherche/dataset/siigsol-100m-carte-des-proprietes-du-sol
Slope Length (L)	Raster	User Generated	1 meter	-
Slope Steepness (S)	Raster	User Generated	1 meter	-
Vegetation Cover (C)	Raster	Données Quebec	30 meters	https://www.donneesquebec.ca/recherche/dataset/carte-ecoforestiere-avec-perturbations
Support Practice (P)	Raster	Données Quebec	30 meters	https://www.donneesquebec.ca/recherche/fr/dataset/utilisation-du-territoire

Objective 1: Revised Universal Soil Loss Equation (RULSE)

Preparing the data

All files listed in the data source table should be downloaded and imported into ArcGIS (Table 1). Each file can be transformed into the size of the area needed through using tools like clip, merge, extract by mask, and mosaic to new raster tools in ArcGIS. Ensure that all files are in the same coordinate systems or have stored meta data that maintains correct projections.

To identify erosion vulnerable crossings, we needed to identify what variables make up soil loss. For this study, we used the Revised Universal Soil Loss Equation (RULSE). Originally, the USLE was used to limit soil resources for agricultural production but has been widely used to detect erosion vulnerabilities (Kinnell, 2010). The Government of Canada (GoC) published recommended guidelines for RULSE that uses a qualitative ranking system to place greater emphasis on the relative implications of soil loss (e.g. severe vs very low impact) and less on calculated soil loss rate. GoC created 5 different soil erosion classes (Very low, low, moderate, high, and severe) along with potential soil loss (tonnes/hectare/year) based on adapted soil loss tolerance level classifications created by Shelton et al. (1985).

It is important to note that Wischmeier & Smith (1978) found that the RULSE tended to overpredict low average annual soil losses, while underpredicting high average annual soil losses. Because of this, we will not be using the exact soil loss predictions to make remediation decisions. Instead, we will classify them into quintiles based on the annual soil loss calculations. Additionally, having a high RULSE index value is a good indicator for erosion prone an area (Wischmeier & Smith, 1978). For this study, we are trying to identify the erosion sites and the severity of them, not estimating how many tons/hectare/year of soil is being lost. An additional reason why we are not using the exact calculations of soil loss annually is because we need to field validate our GIS findings. If we were to use exact numbers, then we would need to measure short- or long-term soil loss measurements over hundreds of sites across several years. By classifying them, we can instead identify the sources of sediment and categorize them by severity, which is easier to measure in the field.

The Revised Universal Soil Loss Equation (RULSE) can be expressed as A = RKLSCP. Where A represents mean annual soil loss (tonnes/hectare/year), R is the rainfall erosivity factor (MJ mm ha^{-1} h^{-1} yr^{-1}), K is soil erodibility factor, L is slope length factor, S is Slope steepness factor, C is crop management factor, and P is erosion control practice factor.

Rainfall erosivity

The relaionship between storm rainfall energy (E) and runoff can vary based on regionality. The rain erosivity factor we use in the RULSE is an empirical rainfall runoff model that Panagos et al. (2023) calculated (Figure 2; Figure 3). The relationship between the two varies more at shorter periods and stabilizes after several years (Foster et al., 2003).

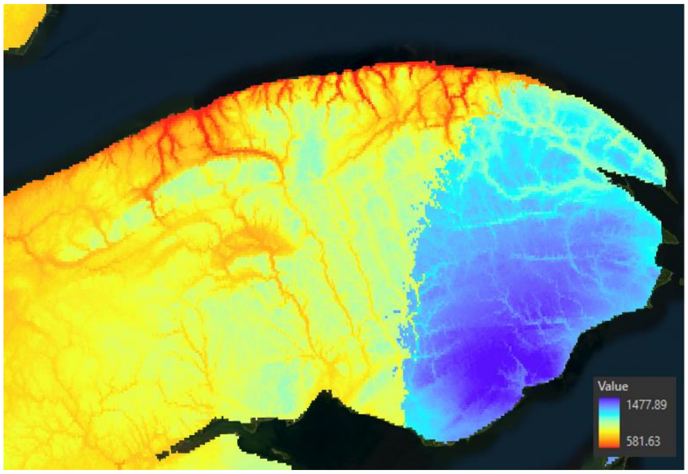

Erosivity is the combination of two rainfall characteristics: kinetic energy and the maximum 30-minute intensity (Kirkby & Morgan, 1980).

Rain Erosivity can be expressed as a factor

$$R_j = E_j \times I_{j30} = \sum_{i=1}^{T_i} (e_i P_{ji}) \times I_{j30}$$

Where:
E_j is kinetic energy (MJ/mm)
I_{j30} is the maximum 30-min rainfall intensity (mm/h)
E_i is unitary kinetic energy (MJ/mm*ha)
P_{ji} is rainfall amount (mm)
T_i is total rainfall duration

Figure 2. Rainfall erosivity raster of the Gaspe Peninsula, Quebec. Data sourced from Panagos et al. (2023).

Rainfall erosivity could be adjusted to potentially increase accuracy by sonidering the relationship between longer term rainfall erosivity (30 years) and the power of event rainfall amount (Bullock et al., 1989).

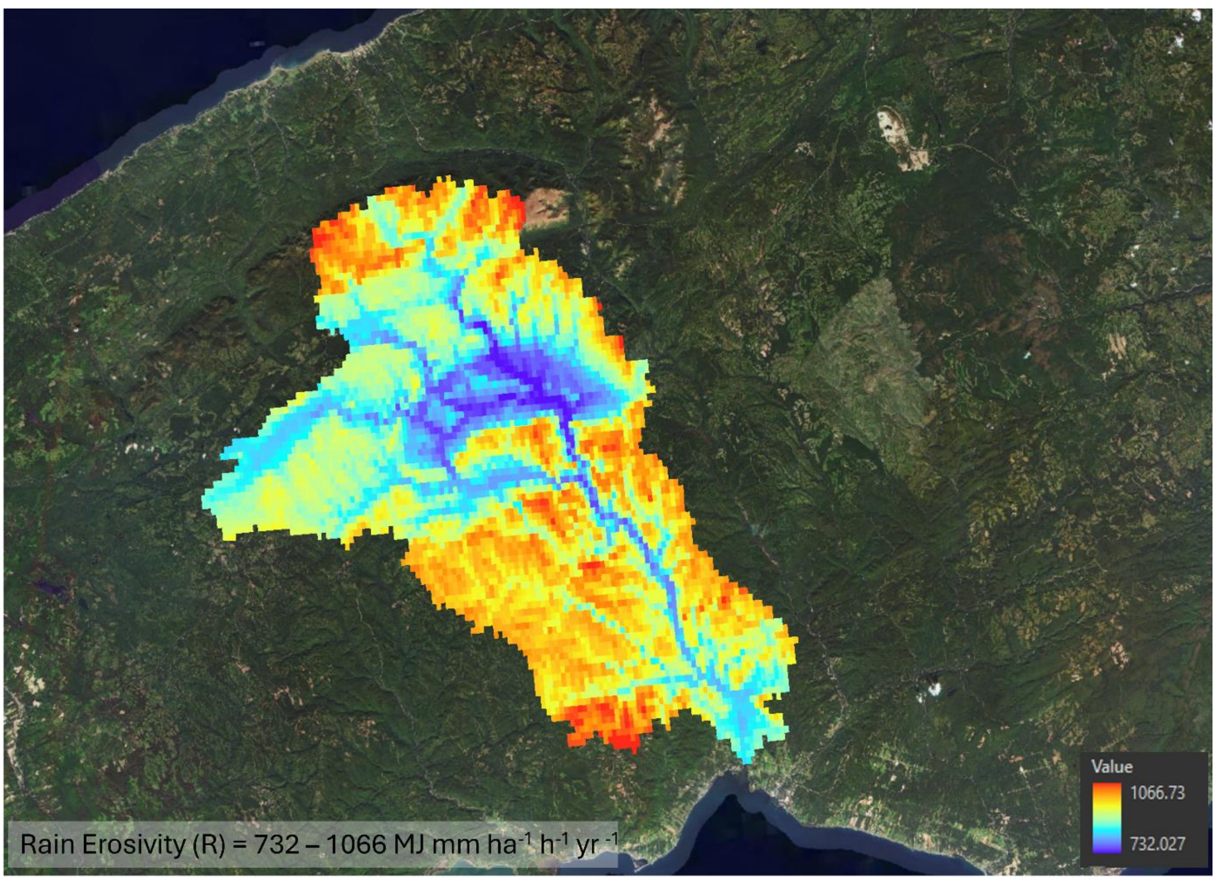

Figure 3. Rainfall Erosivity of the Cascapedia watershed.

Soil erodibility factor

The next step is to estimate soil erodibility based on soil texture and organic material. Soil erodibility factor (K), is a quantitative measure of a soil's inherent susceptibility and resistance to erosion and the soul's inmfluence on runoff amount and rate. In the absence of field tests, these calues can be estimated using relationships based on physical and chemical properties. A soil textural class table will be used in this study. There are numerous tables to estimate K, I used a combination of Roose (1996) and I used regional sources from Donnes Quebec if they were avaialble (Figure 4). The table includes textural class, soul composition, and mean K (Table 2). Some tables account for the percentage of organic matter, not just the organic carbon that was in step 4.

Table 2., Soil erodibility table based on soul composition. Table is sourced directly from Roose (1996).

Estimating soil erodibility (K) based on soil texture and organic material content.

Textural Class	Spanish Texture Class	Soil composition			Mean K (based on % organic material)		
		Sand	Silt	Clay	unknown	< 2%	≥ 2 %
Clay	*Arcilloso*	0-45	0-40	40-100	0.22	0.24	0.21
Sandy Clay	*Arcilloso arenoso*	45-65	0-20	35-55	0.2	0.2	0.2
Silty Clay	*Arcilloso limoso*	0-20	40-60	40-60	0.26	0.27	0.26
Sand	*Arenoso*	86-100	0-14	0-10	0.02	0.03	0.01
Sandy Loam	*Franco arenoso*	50-70	0-50	0-20	0.13	0.14	0.12
Clay Loam	*Franco - arcilloso*	20-45	15-52	27-40	0.3	0.33	0.28
Loam	*Franco*	23-52	28-50	7-27	0.3	0.34	0.26
Loamy Sand	*Franco arenoso*	70-86	0-30	0-15	0.04	0.05	0.04
Sandy Clay Loam	*Franco arenso arcilloso*	45-80	0-28	20-35	0.2	0.2	0.2
Silty Clay Loam	*Franco limoso arcilloso*	0-20	40-73	27-40	0.32	0.35	0.3
Silt	*Limoso*	0-20	88-100	0-12	0.38	0.41	0.37
Silty Loam	*Franco limoso*	20-50	74-88	0-27	0.38	0.41	0.37

To convert organic carbon to organic matter, the equation is as follows: Organic matter = 1.72 * OC (IPCC-AFOLU, 2006). When you determine the textural class, you can calcualte the soil erodibility factor using your calculated organic matter (Table 2; Table 3).

Table 3. Soil type ID's with the percentage of sand, silt, clay, and organic carbon for each soil class which was used to calculate organic material (%), texture class, and soil erodibility (K).

Soil ID	Sand (%)	Silt (%)	Clay (%)	Organic Carbon (%)	Organic Material (%)	Texture Class	Soil Erodibility (K)
3463	54	40	6	7.217	12.41324	Sandy Loam	0.016
4629	43	46	11	4.708	8.09776	Loam	0.038
4949	54	40	6	7.217	12.41324	Sandy Loam	0.016
6708	58	37	5	2.221	3.82012	Sandy Loam	0.016

The output from the above steps should output a classified raster based on soil erodibility (Figure 4).

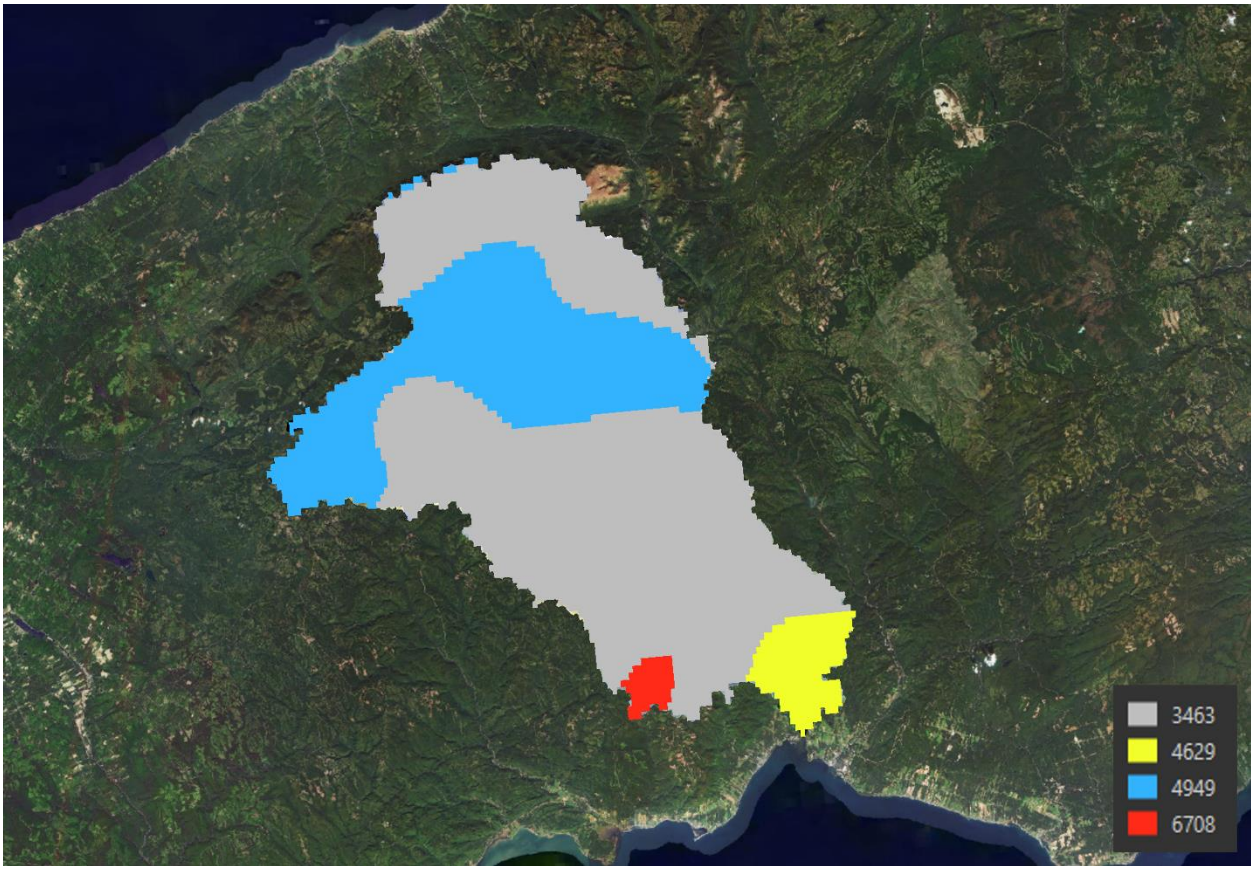

Figure 4. Soil textural class classification based on the proportion of sand, silt, clay, and organic material.

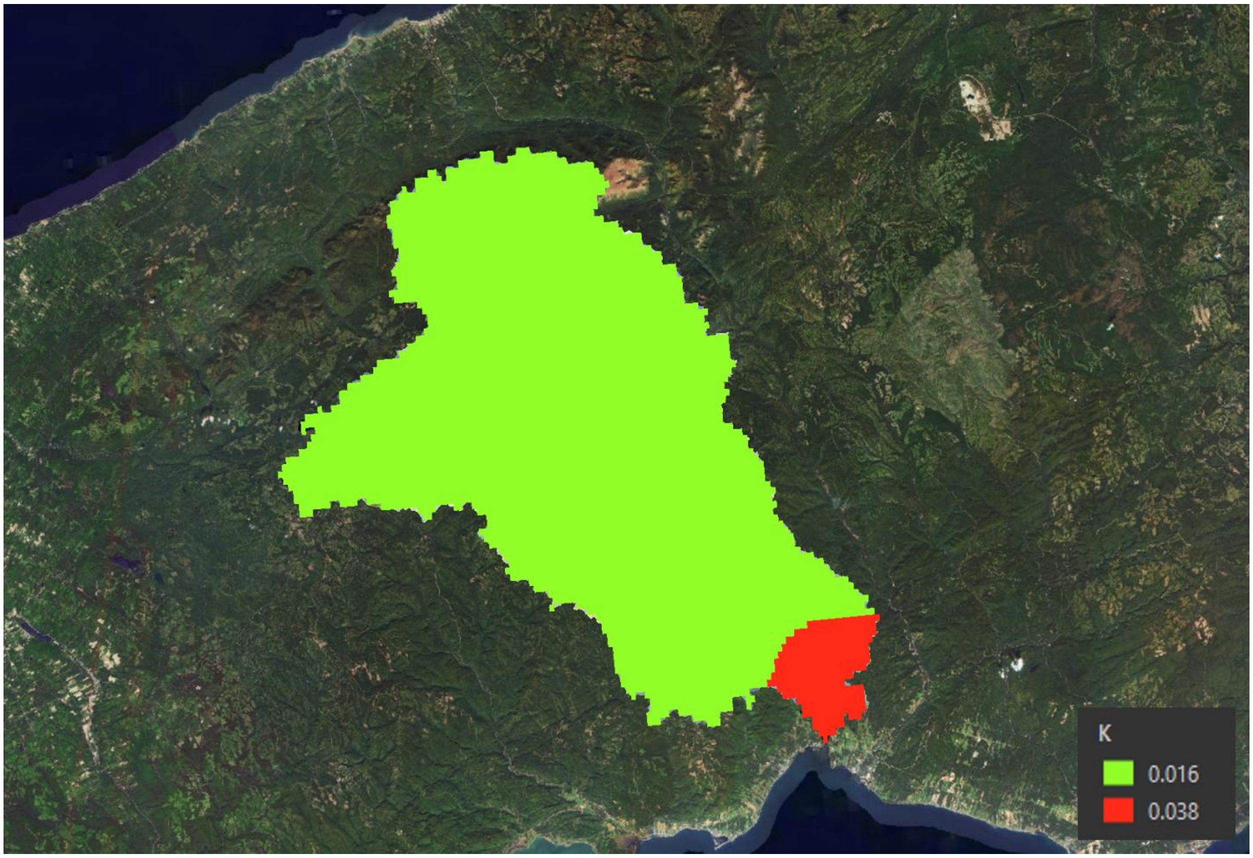

Figure 5. Soil erodibility factor (K).

Length and steepness of slope factor

The length and steepness of slope factor accounts for the effects of slope angle and length on erosion (Figure 5). For example, as the slope length (L) increases, erosion increases, due to the accumulated runoff direction of a downward slope. As slope steepnes (S) increeases, erosion potential increases due to the increased velocity of runoff. When calculating the length-slope factor (LS), a The RULSE is a unit plot concept, so we defined it as a tilled bare fallow area that would be set as 22.1 meters long, on a 9% slope (Moore and Wilson, 1992). Other studies have chosen other length or slopes based on regionality, landscape morphology, or due to modifications of the RULSE (Foster et al., 2003). The LS factor can be expressed as the following:

$$LS = \left(flow\ accumulation \times \frac{Cell\ Size}{22.13}\right)^{0.5} \times \frac{Sin\ (Slope)^{1.3}}{0.0896}$$

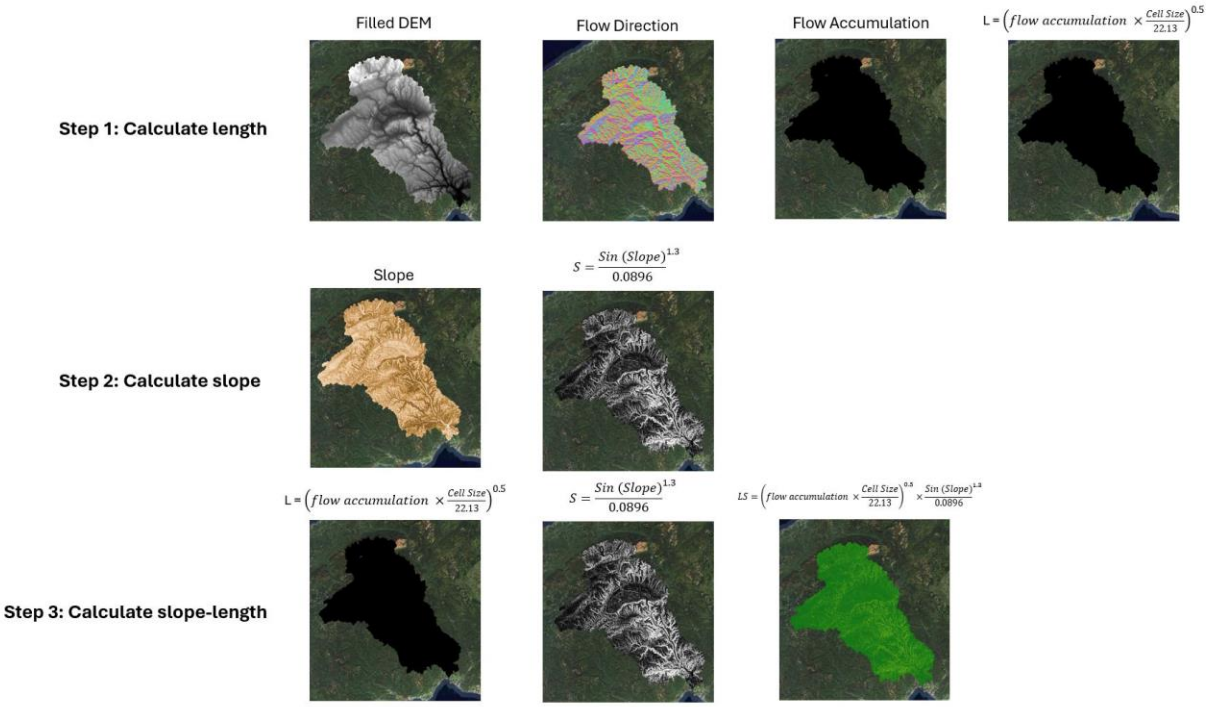

Figure 6. First step: hydro conditioning DEM and calculating the length (L) for the RULSE equation. Second step: calculating slope (S). Third step: Calculate Slope-Length (LS).

Where LS is the length slope factor, cell size is the resolution of your DEM, and the remaining variables are static, but can vary depending on which literature or methodology bests fits the region, for our study we used Moore and Wilson (1992) calculations. The output will be a raster representing the length and steepness of slope factor (Figure 6; Figure 7).

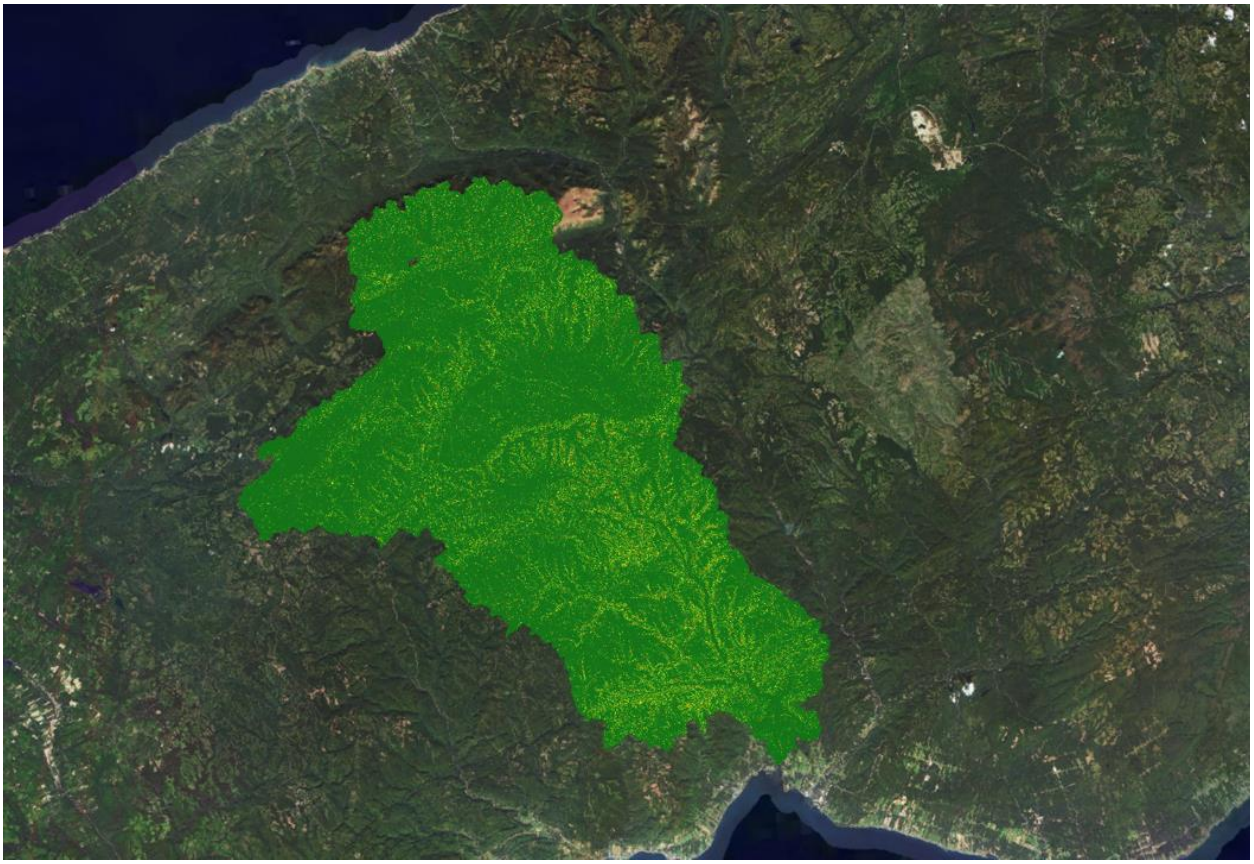

Figure 7. Length and steepness of slope factor (LS).

Crop and management factor (C)

The crop management factor is used to determine the effectiveness of soil and crop management in preventing soil loss. These variables can be found in land use layers sourced from Donnes Quebec and assigned to different land use/cover values based on the land type (Table 4; Figure 8).

Table 4. Land use classification and the corresponding C values.

Land classification	C Value
Agriculture	0.05
Forest	0.002
Wetland	0.05
Water	0
Anthropogenic	1
Cutting and regeneration	0.02
Bare soil	0.35

After the land use classes are assigned C-values, the land use index raster can be transformed using the classify function to display land use based on C-values (Figure 8).

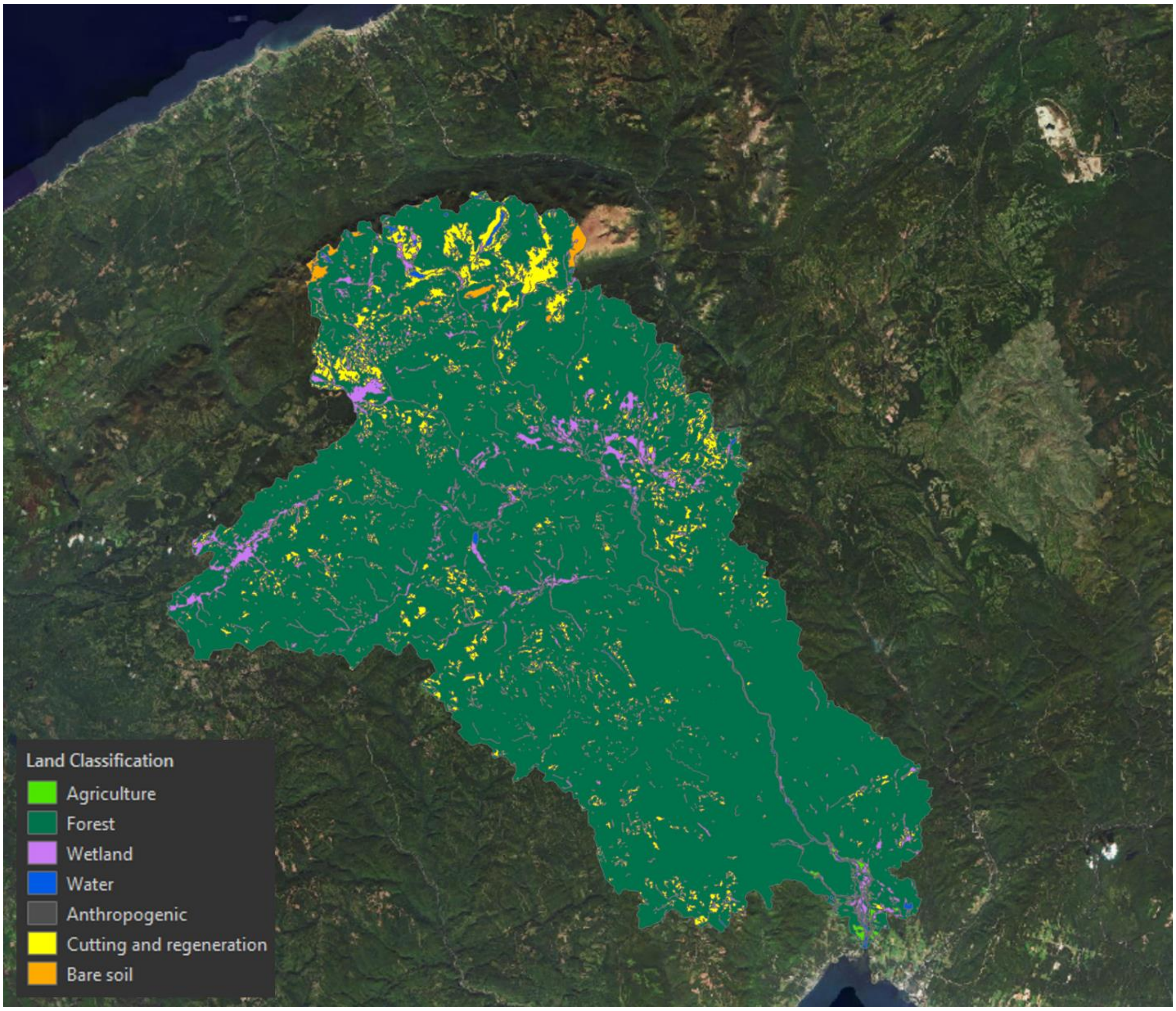

Figure 8. Land use map expressed as C-values.

Support practice factor (P)

The support practice factor is used to account for the support practice factor which can be used to classify erosion control effectiveness. Unfortunately, many regions do not have this data, including Quebec. In cases like these, a value of 1 will be assigned to P, which results in no change or alterations to the output of the RULSE.

RULSE Output

After all layers have been created, they can be combined by using the original equation A = RKLSCP. Using the raster calculator tool, you can multiply all the layers into a signal raster that will result in soil loss expressed as tonnes/hectare/year. The GoC adapted a methodology for their estimated annual soil loss from an analysis done by Shelton et al., (1985). Shelton et al., (1985). The field data for the GoC calculations were collected mainly from Ontario and warned that the estimated annual soil loss amounts should not be taken as a fact. For our methodology, we will not be using the estimated annual soil loss categories from the GoC due to differing landscape characteristics, top-soil depths, soil group types, annual rainfall, and organic matter composition. We wanted to measure watershed specific erosion severity; framing the data to represent how erosion-prone an area is relative to the watershed. To accomplish this, we split the data into quintiles to display relative erosion severity across the watershed (Table 5; Figure 9).

Table 5. Quintile ranges for RULSE raster output.

Soil Erosion Class	Quintile Ranges
Very Low (1^{st} Quintile)	0 - 19.99%
Low (2^{nd} Quintile)	20 - 39.99%
Moderate (3^{rd} Quintile)	40 – 59.99%
High (4^{th} Quintile)	60 – 79.99%
Severe (5^{th} Quintile)	80 – 100%

Figure 9. Universal Soil Loss Equation raster categorized by quintiles.

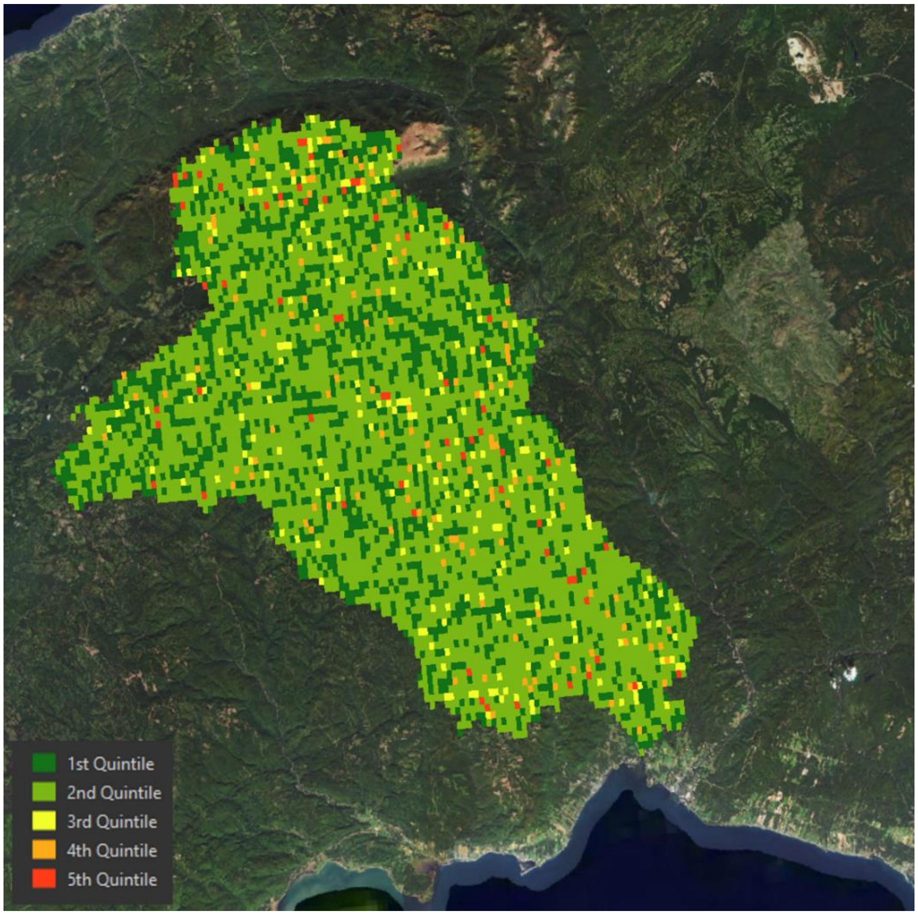

Objective 2: Identify erosion-prone stream crossings and use the sediment transport index to identify sediment sources

Identifying erosion-prone stream crossings

Once the user has the RULSE raster, they will use the “Intersect” or “Pairwise Intersect” tool in ArcGIS, with the inputs being your road and stream network. The intersect tool will create a point wherever the road and stream polylines cross each other.

The next step is to identify what potential crossings are within the upper quintiles (most erosive potential). This can be done by using the “Raster to Polygon” tool on your RULSE raster to create a shapefile of the higher erosive areas (Figure 10). After, you can use the “Clip” tool to create a new point shapefile that only includes the stream crossings within higher erosive areas.

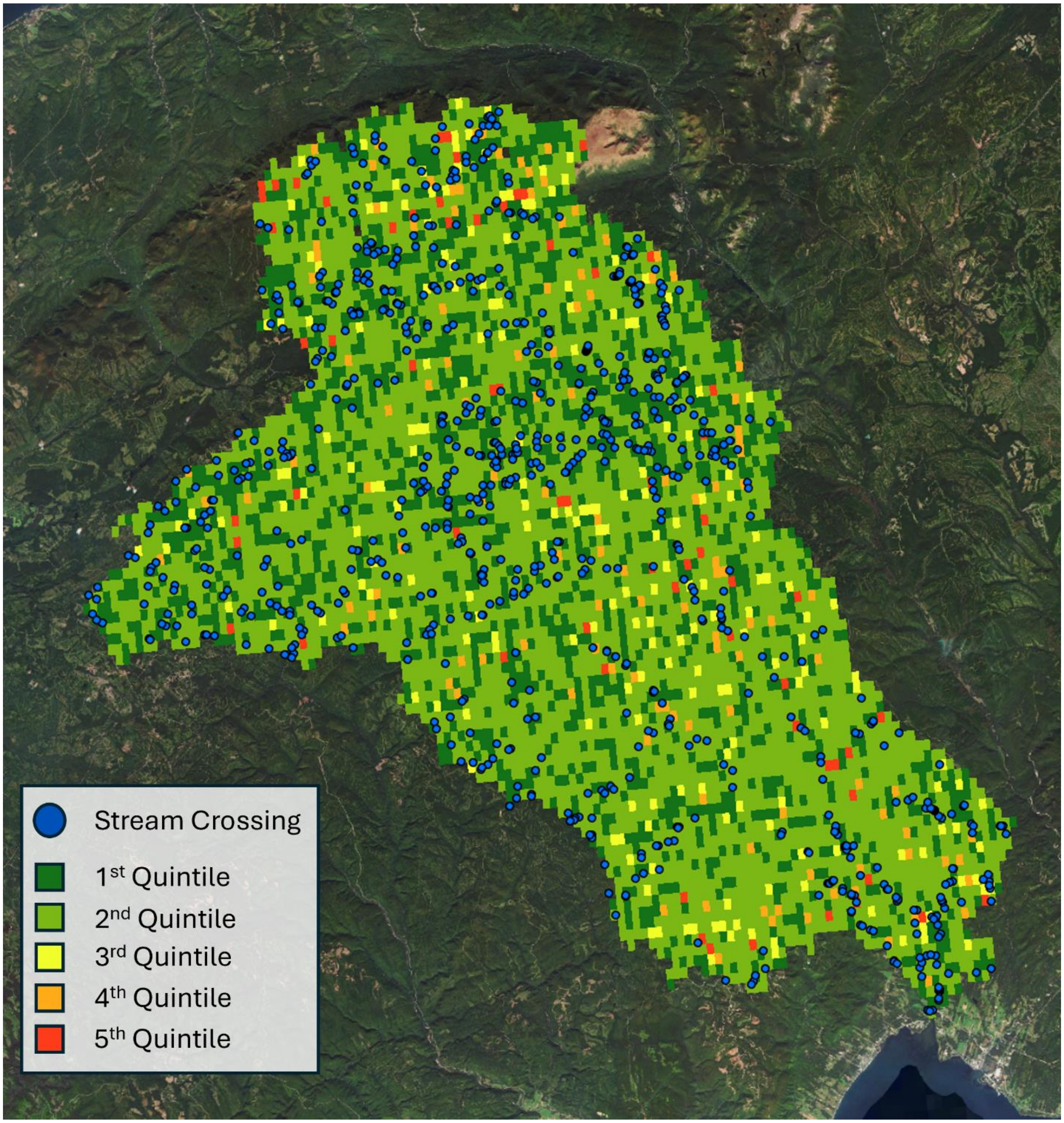

Figure 10. Universal Soil Loss Equation raster categorized by quintiles overlaid with stream crossing locations.

Sediment Transport Index

The Sediment Transport Index (STI) measures the capability of water flow to transport sediments. The sediment transport index by Moore & Burch (1986) can be expressed as:

$$STI = (m + 1) \times (As / 22.13)m \times sin(B / 0.0896)n$$

Where As is the specific catchment area, B is, the local slope gradient in degrees, m is set to 0.6 and n is set to 1.3 (Wischmeyer, 1978).

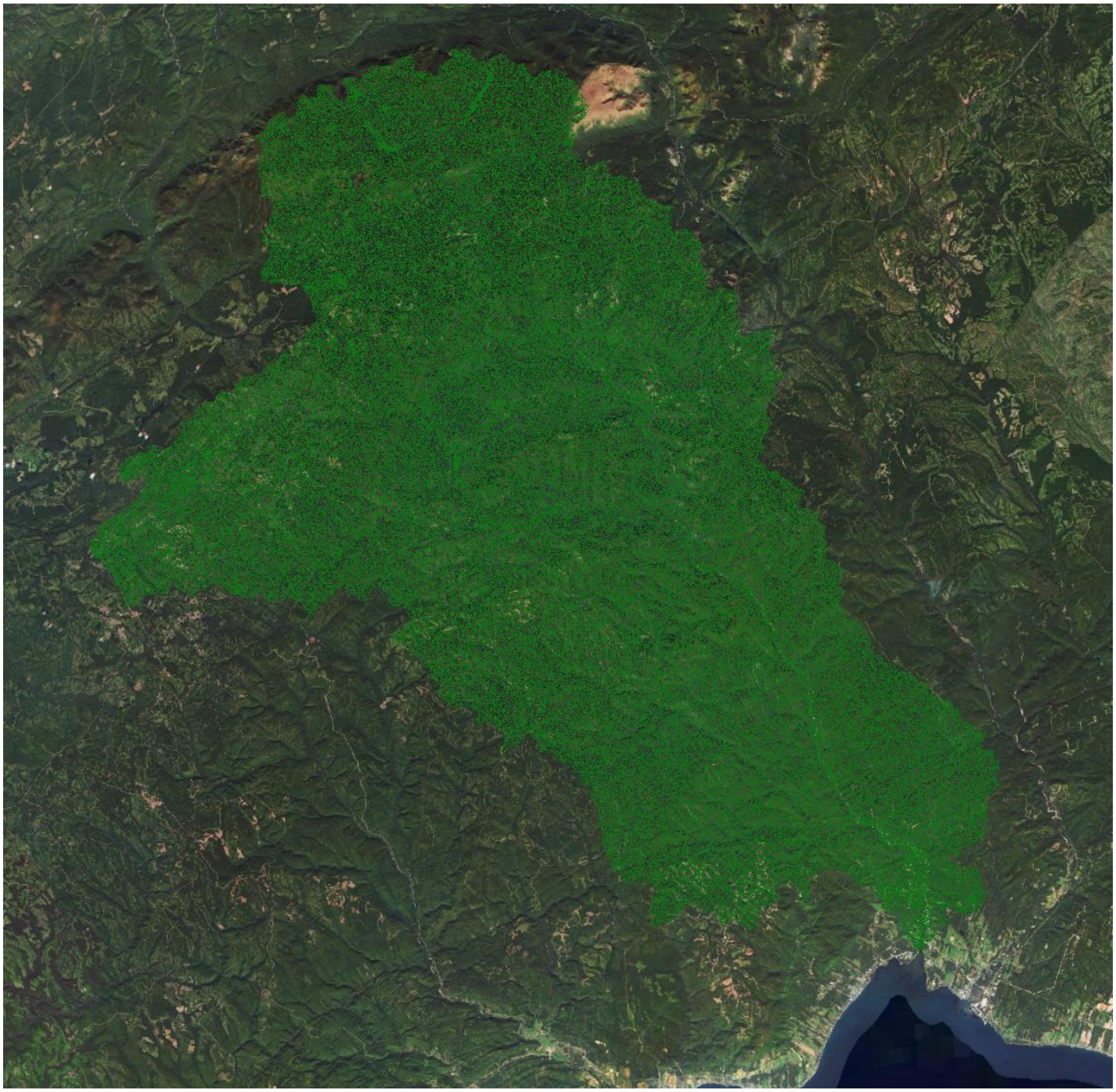

Figure 11. Sediment Transport Index (STI) raster

This equation above can be run in the "Raster Calculator" tool in ArcGIS and would be expressed as:

$$Power\ (\text{“}SCA\text{”}/22.13, 0.16)\ *\ Power\ (Sin(\text{“}Slope.tif\text{”})\ /\ 0.0896{,}1.3)$$

The output will be a dimensionless sediment transport index raster where high values indicate high potential sediment travel while low values indicate low potential for sediment transport (Figure 11).

After a site is chosen (Figure 12), use your sediment transport index to determine what flow paths have the highest likelihood of carrying that sediment. Each crossing will have to be inspected manually like our field verification methods. If all layers are completed and no additional processes are needed, a user can locate the erosive flow paths and identify what landscape feature it is within a minute; expect 1-2 minutes per site for a novice ArcGIS user.

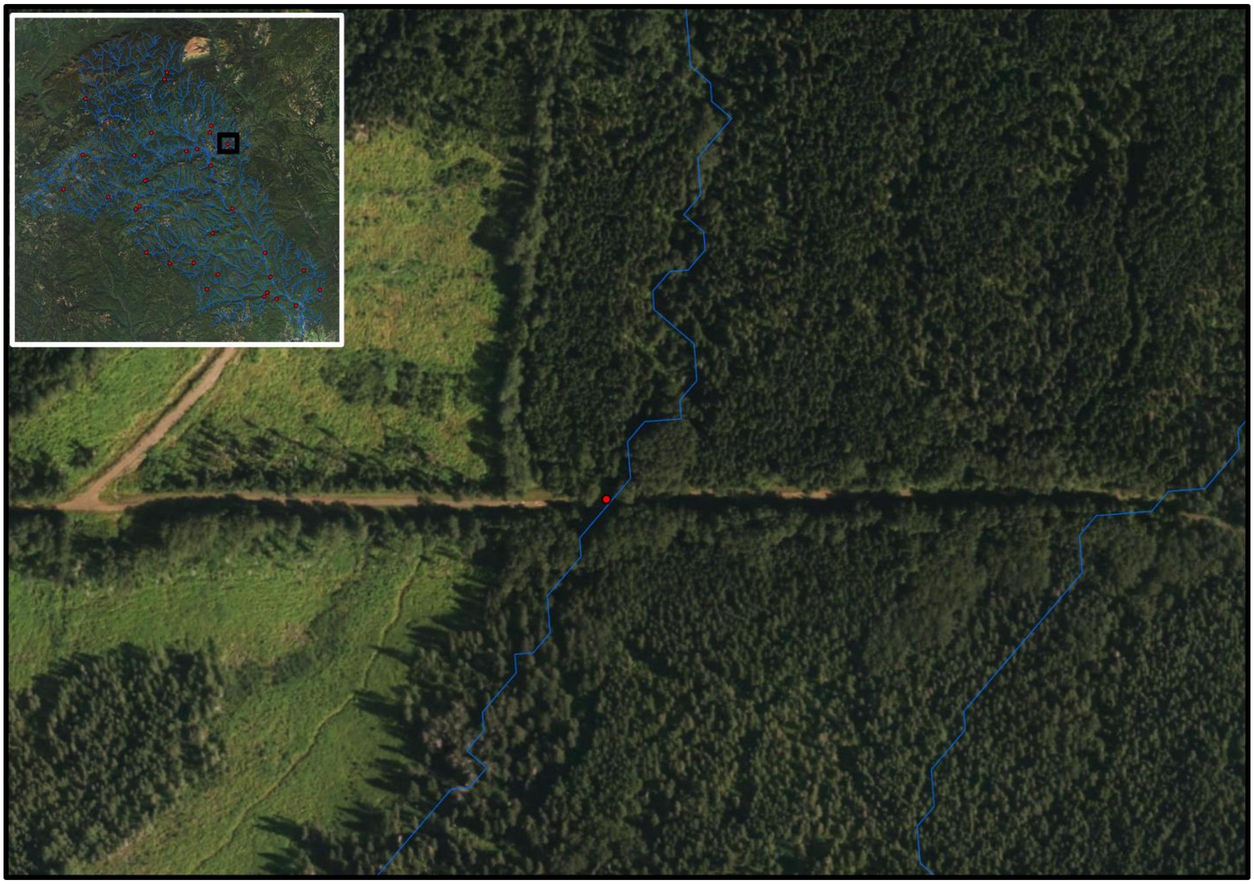

Figure 12. Stream crossing that was flagged as erosion-prone.

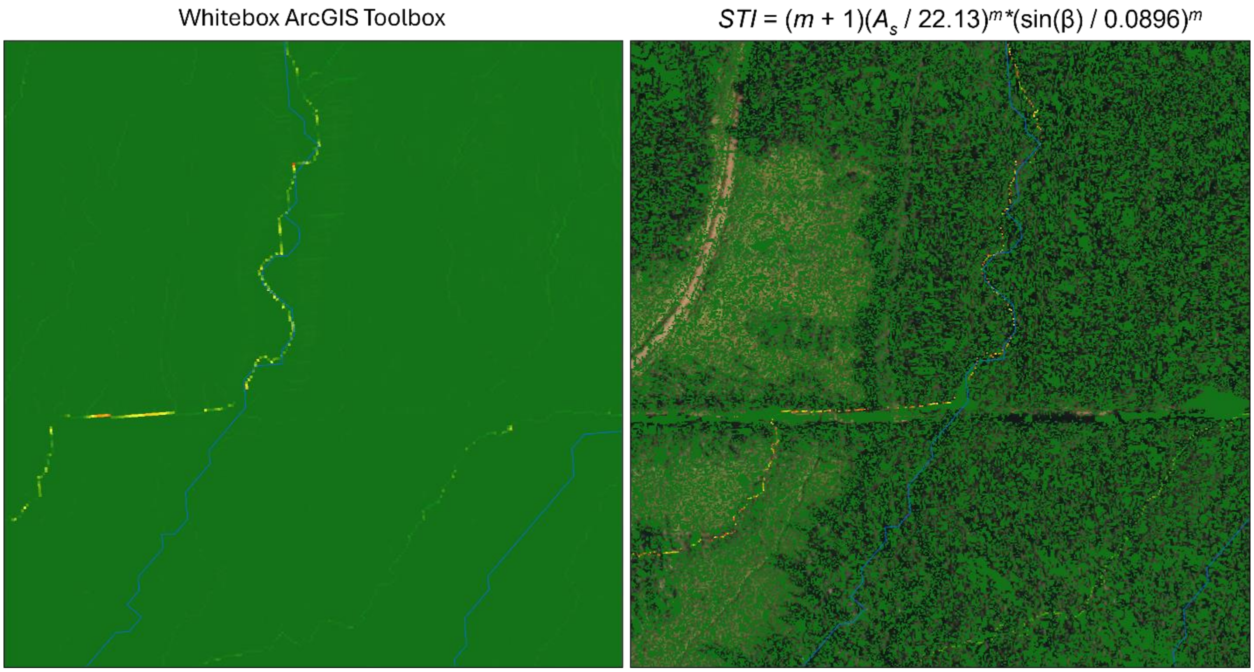

Figure 13. STI rasters created from two separate approaches, the left from Whitebox ArcGIS toolbox, the right using standard methodology.

Figure 13 shows two methods of the sediment transport index identified similar sediment paths. The stream in this example flows from the North to the South and the elevation increases from East to West. The STI shows that as the water flows south, it is redirected from its natural flow path across the road and creating a gully to the Southwest. The orthophotography further reinforces these claims, showing that the sediment path follows the ditch line, across the road, and down into the gully. With these observations, we could assume that the culvert is not operating properly, whether it be from hanging, failure, or blockage if the flow paths are being redirected into the road. To further reinforce these claims, the culvert was digitized using Arsenault et al. (2022) methodology to get the estimated elevation difference between the up and downstream end of the culvert (m) and the slope of the culvert (%). The elevation difference is 0.33 meters, and the slope is approximately 2.5%. According to Anderson et al. (2012), culverts that have more than a 0.3-meter elevation difference have a high likelihood of being a hanging culvert.

Objective 3: Field Verification

Field site selection

To determine which sites are erosion prone, we selected the upper two quintiles as an indicator that the areas are the most severe erosion cases relative to the watershed. We were able to identify erosion-prone stream crossings. Of the 37 stream crossings, 22 are culverts, 4 are bridges. 9 are fords, and 2 were impoundments. Of the 37 crossings, 29 (78%) were located on dirt roads. If we were to expand the analysis to the upper three quintiles, the number of erosion sites would be approximately 71 sites (Table 7).

For field work variable examples, please refer to "Appendix A: Field work data collection examples".

Variables measured

Table 6. Field variables measured, the data type, and what it measures.

Variable	Qualitative or Quantitative?	Measurement
Stream crossing type	Qualitative	Culvert, bridge, ford, impoundment
Crossing characteristics	-	Condition of the stream crossing structure (failure, blockage, hanging)
Road surface material	Qualitative	Paved or Dirt
Road shape	Qualitative	Shape of road (crown, inslope, outslope)
Up/downstream road embankment erosion	Qualitative	Percentage of the road embankment that shows evidence of erosion
Sediment source	Qualitative	Rill/rut from road surface, gully, hanging culvert, undercut culvert, road embankment, stream embankment
Channel constriction	-	Percentage the stream narrows at the stream crossing structure
Road slopes	Quantitative	% slope rises from the stream crossing to the crest of the road

After sites were identified, we compared our field data collected in November 2024 to our identified sites. We are not measuring erosion rates, but presence and source of erosion at the stream crossing. For each site on GIS, the location and type of sediment source (Table 6) were recorded, which were then compared with the GIS results (Table 8).

For an expanded results section that includes areas outside of the Casacapedia watershed, please refer to "Appendix A: Field work data collection examples" for a more robust comparison across the Gaspe Peninsula.

Table 7. Crossing type, the number of each crossing type, and the number of crossings that are within erosion prone areas flagged by the RULSE.

Crossing Type	N	Crossings vulnerable to erosion
Culvert	183	22
Bridge	68	4
Ford	78	9
Impoundment	19	2

We identified 22 different sediment sources at stream crossing for the 8 stream crossings within the Cascapedia watershed. In comparison, our GIS methodology detected 25 sediment sources (Table 7). Field surveys showed 4 gullies, 4 rill/rut, 3 culvert, 3 road embankment, and 5 stream embankment sediment sources (Table 8). Our GIS methodology identified 8 gullies, 7 rill/rut, 3 culvert, 3 road embankment, and 4 stream embankment sediment sources (Table 8). Our methodology over predicted rill/rut erosion and gullies the most, which could be caused by the flow paths being redirected due to road embankments; a more thorough explanation will be discussed in the "Objective 4".

Table 8. GIS and Field sediment source identification. Data is separated into individual crossings and the type and number of sediment sources per crossing.

Crossing #	GIS					Field				
	Gully	Rill/Rut	Culvert	Road embankment	Stream embankment	Gully	Rill/Rut	Culvert	Road embankment	Stream embankment
1	1	1	0	0	0	1	1	0	0	0
2	1	1	1	0	1	1	1	0	0	1
3	1	0	0	1	2	1	0	0	1	2
4	1	1	0	0	0	0	1	1	0	0
5	1	1	1	1	0	0	1	1	1	0
6	0	1	0	0	0	0	1	0	0	0
7	2	1	0	1	0	1	1	0	1	0
8	1	1	1	0	1	0	1	1	0	2

For an expanded results section that includes areas outside of the Casacapedia watershed, please refer to "Appendix B" for a more robust comparison across the Gaspe Peninsula.

Objective 4: Project Outcome

Our study within the Cascapedia watershed and the expanded analysis to the entire Peninsula has shown that we can use high resolution DEM and other publicly data to identify erosion-prone areas at a watershed scale and identify the specific sediment sources for each crossing.

One of the differences between the field and GIS data was that when a user identified a gully or ditch sediment source, the field would either observe the same or, in some cases, there would be no gully erosion, but significant culvert damage. This would be an indication that there is a culvert failure or blockage causing the stream flow to redirect to a gully and crossing the road, which would result in rill/rut erosion. On the other side, if we are overestimating sediment sources, it could be due to an unresolved depression in the DEM causing the flow to redirect across the road. The latter would be less likely due to the hydro conditioning of the DEM during data preparation. Additionally, if there was a depression or some artifact that affected the flow pathing, then it would be present within the hydro conditioned DEM, which we found no instances of in this project.

Our methodology will continue to develop as we learn more and incorporate more field data to better understand how we can adjust our methodology to best fit the needs of the user. Our next steps are to expand the analysis to the entire Gaspe Peninsula and integrate more field sites. Additionally, once all data has been compiled, we will be working on how to prioritize the restoration of the sites, potentially create a toolbox to automate some steps, and provide the data on an online mapping service for easier access and customizability.

References

Anderson GB, Freeman MC, Freeman BJ, Straight CA, Hagler MM, Peterson JT. Dealing with uncertainty when assessing fish passage through culvert road crossings. Environ Manage. 2012 Sep;50(3):462-77. doi: 10.1007/s00267-012-9886-6.

Arsenault, M., O'Sullivan, A. M., Ogilvie, J., Gillis, C. A., Linnansaari, T., & Curry, R. A. (2022). Remote sensing framework details riverscape connectivity fragmentation and fish passability in a forested landscape. *Journal of Ecohydraulics*, *8*(2), 121–132. https://doi.org/10.1080/24705357.2022.2040388

Argent, D. G., and P. A. Flebbe. (1999). Fine sediment effects on brook trout eggs in laboratory streams. Fisheries Research 39:253–262.

Biron, P. M., Choné, G., Buffin-Bélanger, T., Demers, S., & Olsen, T. (2013). Improvement of streams hydro-geomorphological assessment using LiDAR DEMs. Earth Surface Processes and Landforms, 38(15), 1808–1821. doi:10.1002/esp.3425

Boston, K. (2016). The Potential Effects of Forest Roads on the Environment and Mitigating their Impacts. *Curr Forestry Rep* **2**, 215–222.

Bullock, PR., de Jong, E., Kisd, J.J., 1989. An assessment of rainfall erosion potential I southern Saskatchewan from daily rainfall records. Canadian Agricultural Engineering 32, 17–24.

Clarke, K.D. & Scruton, D.R. (1997) The Benthic Community of Stream Riffles in Newfoundland, Canada and its Relationship to Selected Physical and Chemical Parameters, Journal of Freshwater Ecology, 12:1, 113-121.

Forman, R.T.T., and Alexander, L. (1998). Roads and their major ecological effects. Annu. Rev. Ecol. Syst. 29(1): 207–231.

Forman, R.T.T., Sperling, D., Bissonette, J.A., Clevenger, A.P., Cutshall, C.D., Dale, V.H., Fahrig, L., France, R., Goldman, C.R., Heanue, K., Jones, J.A., Swanson, F.J., Turrentine, T., and Winter, T.C. (2003). Road ecology: science and solutions. Island Press, Washington, DC. 481 p.

Foster, G.R., Toy, T.E., Renard, K.G., 2003. Comparison of the USLE, RUSLE1.06 and RUSLE2 for application to highly disturbed lands. In: Renard, K.G., Mc. Ilroy, S.A., Gburek, W.J., Cranfield, H.E., Scott, R.L. (Eds.), First Interagency Conference on Research in Watersheds, October 27–30, 2003. US Department of Agriculture.

Fu, B., Lachlan T.H. Newham, C.E. Ramos-Scharrón. (2010). A review of surface erosion and sediment delivery models for unsealed roads, Environmental Modelling & Software, Volume 25, Issue 1, Pages 1-14.

Kastridis, A. (2020). Impact of Forest Roads on Hydrological Processes. *Forests*.

Kemp PS, O'Hanley JR. 2010. Procedures for evaluating and prioritizing the removal of fish passage barriers: A synthesis. Fish Manag Ecol. 17:no–322.

Kinnell, P. I. A. (2010). Event soil loss, runoff and the Universal Soil Loss Equation family of models: A review. Journal of Hydrology, 385(1-4), 384–397. doi:10.1016/j.jhydrol.2010.01.024

Lohani, Bharat & Ghosh, Suddhasheel. (2017). Airborne LiDAR Technology: A Review of Data Collection and Processing Systems. Proceedings of the National Academy of Sciences, India Section A: Physical Sciences. 87. 10.1007/s40010-017-0435-9.

Mobtaker, A., Ouhimmou, M., Rönnqvist, M., & Paquet, M. (2018). Development of an economically sustainable and balanced tactical forest management plan: a case study in Quebec. Canadian Journal of Forest Research, 48(2), 197–207. doi:10.1139/cjfr-2017-0232.

Moore, I.D. & Wilson, John. (1992). Length-slope factors for the revised universal soil loss equation: simplified method of estimation. Journal of Soil & Water Conservation. 47. 423-428.

Nelson, J. (2010). Digital Terrain Analysis with LiDAR for Clean Water Implementation – Workshop April 7, 2010. Minnesota Department of Agriculture. Acquired during MN Dept. of Ag. Workshop in Winona, MN April 7, 2010.

Panagos, Panos & Borrelli, Pasquale & Poesen, J. & Ballabio, Cristiano & Meusburger, Katrin & Montanarella, Luca & Lugato, Emanuele & Alewell, Christine. (2015). The new assessment of soil loss by water erosion in Europe. Environmental Science & Policy. 54. 438-447. 10.1016/j.envsci.2015.08.012.

Papangelakis, Elli & MacVicar, Bruce & Ashmore, Peter & Gingerich, David & Bright, Christina. (2022). Testing a Watershed-Scale Stream Power Index Tool for Erosion Risk Assessment in an Urban River. Journal of Sustainable Water in the Built Environment. 8. 10.1061/JSWBAY.0000989.

Prosdocimi, I., Kjeldsen, T. R., and Miller, J. D. (2015), Detection and attribution of urbanization effect on flood extremes using nonstationary flood-frequency models, *Water Resour. Res.*, 51, 4244– 4262

Rice, S. P., and Church, M. (2001), Longitudinal profiles in simple alluvial systems, *Water Resour. Res.*, 37(2), 417– 426, doi:10.1029/2000WR900266.

Robichaud, Peter R.; Brown, Robert E. 2002. Silt fences: an economical technique for measuring hillslope soil erosion. Gen. Tech. Rep. RMRS-GTR-94. Fort Collins, CO: U.S. Department of Agriculture, Forest Service, Rocky Mountain Research Station. 24 p.

Roose, Eric. *Land husbandry: components and strategy*. Vol. 70. Rome: FAO, 1996.

Kevin L. Shelton, John M. Reader, Louis M. Ross, George W. Viele, David E. Seidemann; Ba-rich adularia from the Ouachita Mountains, Arkansas; implications for a post collisional hydrothermal system. *American Mineralogist* 1986; 71 (7-8): 916–923.

Sheridan, G. J., & Noske, P. J. (2007). *A quantitative study of sediment delivery and stream pollution from different forest road types. Hydrological Processes, 21(3), 387–398.*

Simon, A., Rinaldi, M., (2000). Channel instability in the loess area of the midwestern United States. Journal of the American Water Resources Association 36 (1), 133 – 150.

Scrimgeour, G. J., W. M. Tonn, C. A. Paszkowski, and P. M. K. Aku. 2000. Evaluating the effects of forest harvesting on littoral benthic communities within a natural disturbance-based management model. Forest Ecology and Management 126:77–86.

Statistics Canada. (2014). Statcan Canadian International Merchandise Trade Database [online]. Available at http://www5.statcan.gc.ca/cimt-cicm/

Trombulak SC, Frissell CA. (2000). Review of ecological effects of roads on terrestrial and aquatic communities. Conserv Biol. 14(1):18–30.

Wallbrink, P.J. B.P Roddy, J.M Olley. (2002). A tracer budget quantifying soil redistribution on hillslopes after forest harvesting, CATENA, Volume 47, Issue 3, Pages 179-201, ISSN 0341-8162.

Wellman, J. C., D. L. Combs, and S. Bradford Cook. (2000). Long-term impacts of bridge and culvert construction or replacement on fish communities and sediment characteristics of streams. Journal of Freshwater Ecology 15:317–328.

Williams, L. R., C. M. Taylor, M. L. Warren, and J. A. Clingenpeel. (2002). Large-scale effects of timber harvesting on stream systems in the Ouachita mountains, Arkansas, USA. Environmental Management 29:76–87.

Wilson, John & Lorang, M.S. (1999). Spatial models of soil erosion and GIS.

Wischmeier, W. H., & Smith, D. D. (1978). *Predicting rainfall erosion losses : a guide to conservation planning* (Vol. 537). USDA, Science and Education Administration.

Wu, W.; Berhe, T.G.; Ashour, T. Embankments and dams. (2012). In Modern Earth Buildings; Woodhead Publishing: Cambridge, UK; pp. 538–558. B.J Zebarth, H Rees, J Walsh, L Chow, D.J Pennock, Soil variation within a hummocky podzolic landscape under intensive potato production, Geoderma, Volume 110, Issues 1–2, 2002, Pages 19-33, ISSN 0016-7061.

Zhao, L., Zhang, K., Wu, S., Feng, D., Shang, H., & Wang, J. (2020). *Comparative study on different sediment transport capacity based on dimensionless flow intensity index. Journal of Soils and Sediments.* doi:10.1007/s11368-020-02568-5

Appendix A: Field work data collection examples

Variables collected:

- Stream crossing type
- Stream classification
- Crossing characteristics
- Road surface material
- Road shape
- Up/Downstream road embankment erosion
- Sediment sources
- Channel constriction
- Road slopes

Field Season 2024

Variables collected:

- **Stream crossing type**
- Stream classification
- Crossing characteristics
- Road surface material
- Road shape
- Up/Downstream road embankment erosion
- Sediment sources
- Channel constriction
- Road slopes

Field Season 2024

Variables collected:

- **Stream crossing type**
- Stream classification
- Crossing characteristics
- Road surface material
- Road shape
- Up/Downstream road embankment erosion
- Sediment sources
- Channel constriction
- Road slopes

Field Season 2024

Field Season 2024

Variables collected:

- Stream crossing type
- **Stream classification**
- Crossing characteristics
- Road surface material
- Road shape
- Up/Downstream road embankment erosion
- Sediment sources
- Channel constriction
- Road slopes

Field Season 2024

Variables collected:

- Stream crossing type
- Stream classification
- **Crossing characteristics**
- Road surface material
- Road shape
- Up/Downstream road embankment erosion
- Sediment sources
- Channel constriction
- Road slopes

Field Season 2024

Variables collected:

- Stream crossing type
- Stream classification
- Crossing characteristics
- **Road surface material**
- Road shape
- Up/Downstream road embankment erosion
- Sediment sources
- Channel constriction
- Road slopes

Field Season 2024

Variables collected:

- Stream crossing type
- Stream classification
- Crossing characteristics
- Road surface material
- **Road shape**
- Up/Downstream road embankment erosion
- Sediment sources
- Channel constriction
- Road slopes

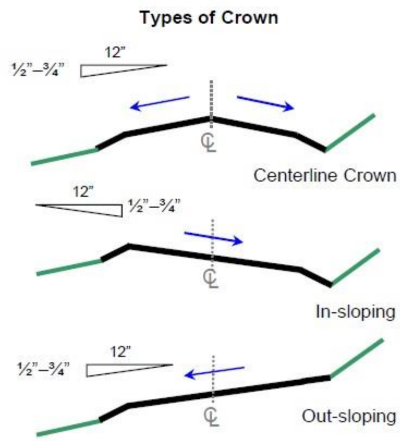

"Crown": Highest elevation point on road is in the center with both sides sloping to the road embankment

"Inslope": Road angle directs flow to a drainage structure/ditch

"Outslope": Road surfaces drain water from the entire width of the road toward the fill bank or down-slope side

Field Season 2024

Road embankment erosion is measured by how much of the road embankment has evidence of erosion, expressed as a %

Variables collected:

- Stream crossing type
- Stream classification
- Crossing characteristics
- Road surface material
- Road shape
- **Up/Downstream road embankment erosion**
- Sediment sources
- Channel constriction
- Road slopes

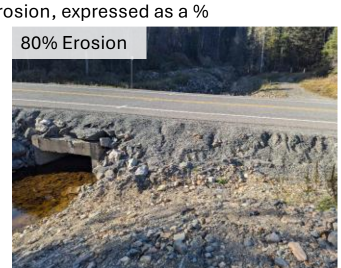

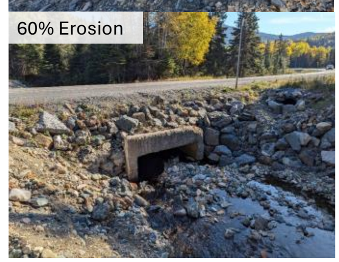

Field Season 2024

Variables collected:

- Stream crossing type
- Stream classification
- Crossing characteristics
- Road surface material
- Road shape
- **Up/Downstream road embankment erosion**
- Sediment sources
- Channel constriction
- Road slopes

Road embankment erosion is measured by how much of the road embankment has evidence of erosion, expressed as a %

Field Season 2024

Variables collected:

- Stream crossing type
- Stream classification
- Crossing characteristics
- Road surface material
- Road shape
- Up/Downstream road embankment erosion
- **Sediment sources**
- Channel constriction
- Road slopes

Field Season 2024

Variables collected:

- Stream crossing type
- Stream classification
- Crossing characteristics
- Road surface material
- Road shape
- Up/Downstream road embankment erosion
- **Sediment sources**
- Channel constriction
- Road slopes

Field Season 2024

Variables collected:

- Stream crossing type
- Stream classification
- Crossing characteristics
- Road surface material
- Road shape
- Up/Downstream road embankment erosion
- **Sediment sources**
- Channel constriction
- Road slopes

Field Season 2024

Variables collected:

- Stream crossing type
- Stream classification
- Crossing characteristics
- Road surface material
- Road shape
- Up/Downstream road embankment erosion
- Sediment sources
- **Channel constriction**
- Road slopes

slope percentage = tan(d) × 100

Field Season 2024

Variables collected:

- Stream crossing type
- Stream classification
- Crossing characteristics
- Road surface material
- Road shape
- Up/Downstream road embankment erosion
- Sediment sources
- Channel constriction
- **Road slopes**

Measure angle from crossing to crest of road, repeat in the other direction

Slope percentage = tan (d) * 100
Where "d" is slope in degrees; not in radian.

Horizontal Distance (Run): 78 meters
Angle: 2 degrees

Slope percentage = tan (2) * 100
Slope percentage = 2.724%

Appendix B: Field data comparison outside of the Cascapedia watershed

Watershed	# of Sediment Sites	# of sediment sources from field (% Accuracy Field vs. GIS)				
		Gully	Rill/Rut	Culvert	Road embankment	Stream embankment
Bonaventure	26	10 (77%)	11 (84%)	9 (89%)	6 (83%)	2 (100%)
Cascapedia	8	4 (50%)	4 (57%)	3 (100%)	3 (100%)	5 (83%)
Little Cascapedia	10	3 (67%)	2 (50%)	4 (75%)	2 (100%)	1 (100%)
Madeleine	2	-	1 (100%)	2 (100%)	1 (100%)	1 (100%)
Nouvelle	23	13 (100%)	26 (90%)	16 (94%)	6 (100%)	5 (100%)
York	4	1 (0%)	4 (100%)	2 (100%)	1 (100%)	1 (100%)